

FULL PAPER

Host–Guest Interactions as a Model for the Solvent Influence on the Conformational Populations in [2.2.2.2]Paracyclophane

Parviz Rashidi-Ranjbar and Nematollah Arshadi

Department of Chemistry, Faculty of Science, Tehran University, Tehran, IRAN. Tel: +98-21- 6495291;
Fax: +98-21-6405141; E-mail: ranjbar@khayam.ut.ac.ir

Received: 11 February 1999/ Accepted: 2 August 1999/ Published: 8 November 1999

Abstract The interaction of a number of small organic molecules with the two lowest energy minimum conformations of [2.2.2.2]paracyclophane (4°-PCP), **1** and **2**, are studied by MMP2(87) force field calculations. Formations of nesting as well as inclusion complexes were identified on the potential energy surface. With CH₂Cl₂ and CHCl₃ used as guests, the nesting complexes are lower in energy than the inclusion ones with both conformations **1** and **2**. Furthermore, the nesting complexes with **2** are found to be more stable than the nesting ones with **1**. Formation of the double nesting complexes of CH₂Cl₂ and CHCl₃ with **1** and **2** raise the difference in complexation energy in favour of **2**. The preference of 4°-PCP for the form **2** in solution is explained based on the above analysis, although **2** is calculated to be 0.2 kcal·mol⁻¹ higher in steric energy than **1** in the gas phase.

Keywords Paracyclophane, Host-guest interactions, Solvent-solute interactions, Force field calculations, Nesting complex, Inclusion complex

Introduction

Molecular recognition plays an important role in many different areas of chemistry as well as molecular biology. The basis of this phenomenon is the ability of a large molecule (host) to recognise and bind small molecules (guests). Understanding the interactions between hosts and guests and the factors that control the stability of those complexes is the main goal in studying molecular recognition phenomena [1-7]. This is important, since the binding of substrates by enzymes and antibodies and transport of ions across bio-

logical membranes occurs in the first step by molecular recognition.

Forces that control the stability of host-guest complexes are non-covalent interactions like hydrogen bonding, van der Waals interactions, dipole-dipole and π -stacking interactions. There is also an additional mode of binding invoked by Cram as “constrictive binding” which is defined as the difference between the activation energy of the dissociation process and the thermodynamic binding energy. It represents the physical barrier that prevents escape of the guest from the host cavity [7].

To study the host-guest complexes and their geometries, X-ray diffraction [8-14], optical [15,16], NMR [15-23] and ESR [24] spectroscopic and computational [13,14,23,25-37] methods are used. Computational tools become increasingly

Correspondence to: P. Rashidi-Ranjbar

important with respect to both the nature of solvophobic interactions and the origins of host-guest interactions [38].

Solvents used for NMR measurements may influence the conformational distribution either by the polarity of the solvent [39,40] or by specific inclusion of a solvent molecule in the cavity of the host [23,41-45]. There might be a possibility that the conformational population be affected by the formation of a nesting complex between the host and solvent molecules. To the best of our knowledge, this type of interaction, the effect of solvent on conformational distribution of the solute, has not been considered yet, nor any possible type of solvophobic interactions. We would like to address the effect of the formation of the nesting complexes on the conformational distribution of [2.2.2.2]paracyclophane (4° -PCP) by force field calculations (see Figure 1a).

Paracyclophanes are an important class of supramolecular compounds with the ability to form inclusion complexes with some guests [17-19]. So far complexation of rigid cyclophanes is studied with different guests [15,16].

In the present study, performed by the MMP2(87) method, we have chosen 4° -PCP as a host and analysed the interaction of different guest molecules by introducing the guest from a far distance to the 4° -PCP cavity and forcing it to pass through the cavity. The whole process could be used as a good model for studying the change in the conformational distributions of the host due to complexation, which makes possible the explanation of the most probable conformation of the host in solution.

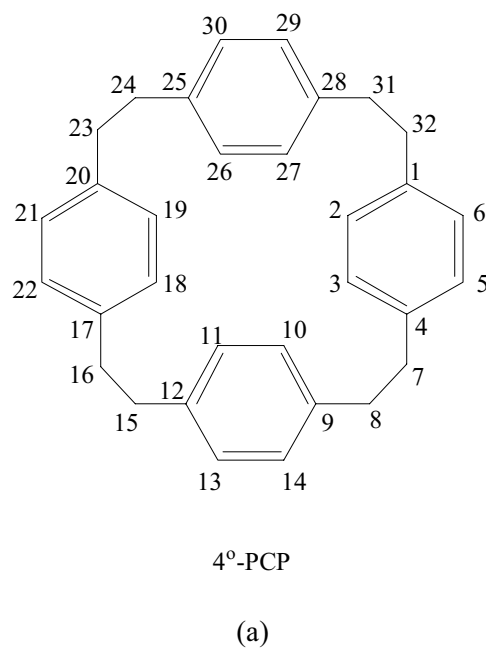


Figure 1a [2.2.2.2]Paracyclophane (4° -PCP)

Figure 1b The two lowest energy minimum conformations of 4° -PCP from two different views (top and side).

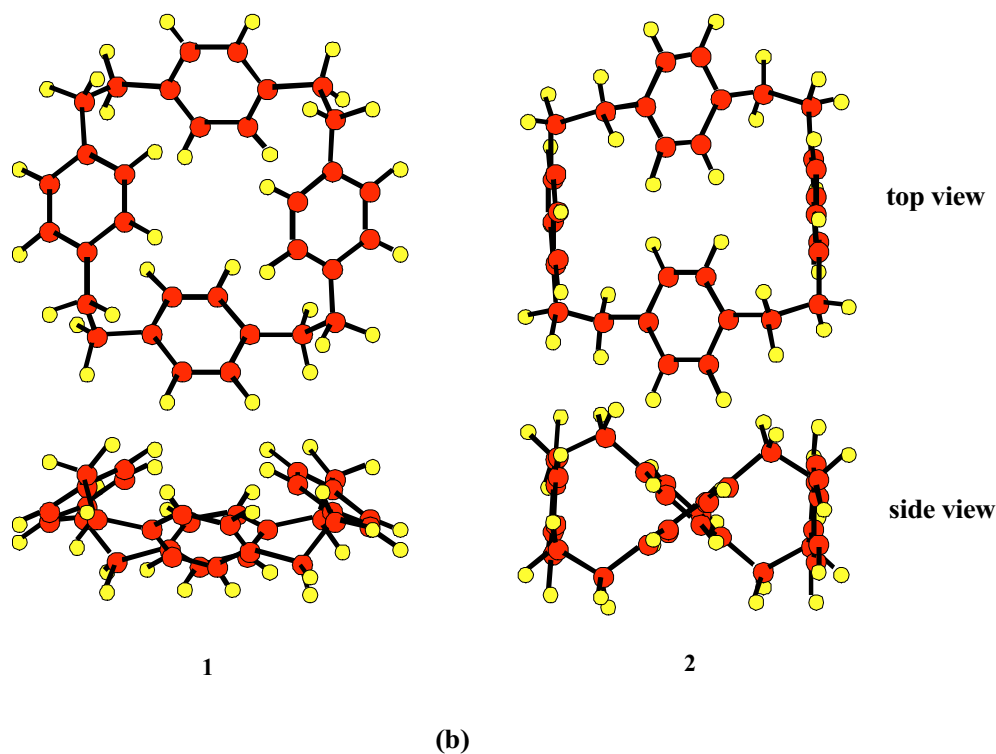


Figure 2 The potential energy surface of interaction of CH_4 as guest with **1**. The inclusion complex is the preferred one. The top and side views of the minimum and maximum energy structures are given. The x-axis refers to the distance between the gravity centre of the guest molecule and the host centre.

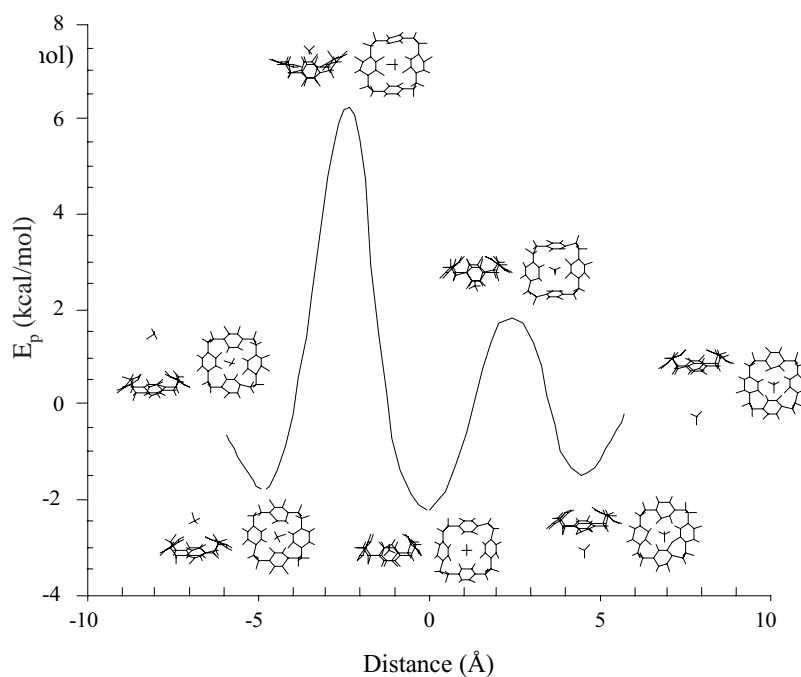
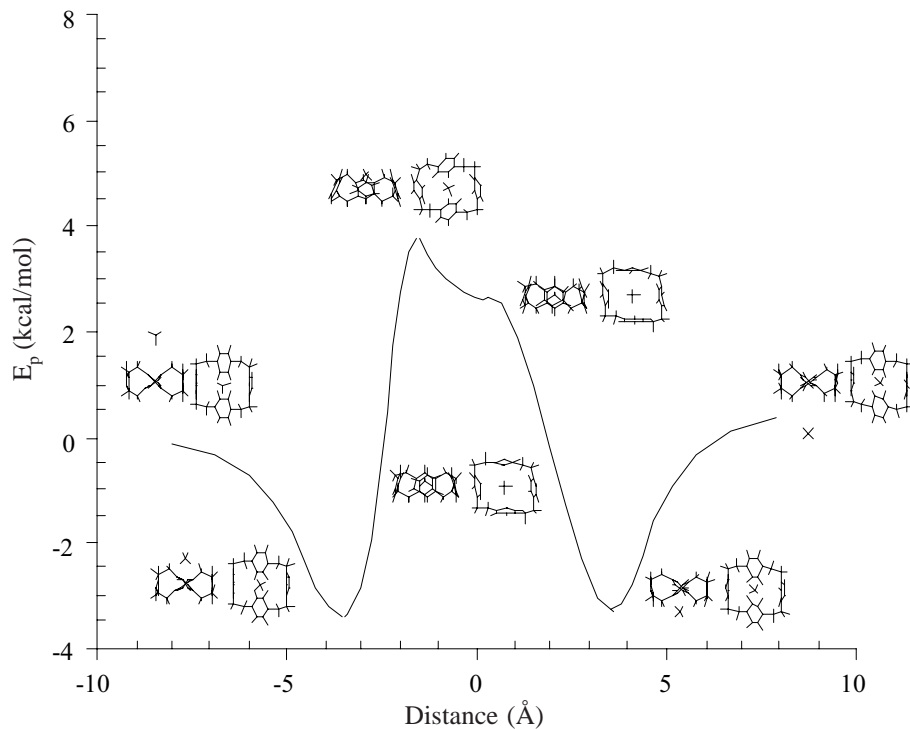


Figure 3 The potential energy surface of interaction of CH_4 as guest with **2**. The nesting complex is the preferred one. The top and side views of the minimum and maximum energy structures are given.



Computational method

Molecular mechanics calculations were carried out using the MMP2(87) force field [46,47]. The performance of the MM2(87) force field is reported to be essentially identical to that of the MM2(91) for conjugated hydrocarbons and alkyl halides [48]. All the energy minimum structures were fully

optimised by the default convergence criterion ($\Delta E < 0.00008$ kcal·mol⁻¹ per atom). The two lowest energy minimum conformations of 4^o-PCP, i.e. **1** and **2** in Figure 1b, that has been explored in a related work [49], were used to investigate the host-guest interactions. In **2** there are two lateral and two facial benzene rings [50], but in **1** benzene rings are neither lateral nor facial. They have been denoted as inclined [49].

Table 1 The dihedral angles of the **1** and **2** conformations of 4^o-PCP; for the numbering see Figure 1

Torsion angle	1	2	Torsion angle	1	2
C(4) - C(7) - C(8) - C(9)	75.0	66.8	C(20) - C(23) - C(24) - C(25)	75.0	66.8
C(5) - C(4) - C(7) - C(8)	96.1	106.1	C(21) - C(20) - C(23) - C(24)	96.2	106.2
C(3) - C(4) - C(7) - C(8)	-84.5	-75.1	C(19) - C(20) - C(23) - C(24)	-84.3	-75.0
C(14) - C(9) - C(8) - C(7)	73.2	66.6	C(26) - C(25) - C(24) - C(23)	-107.3	66.6
C(10) - C(9) - C(8) - C(7)	-107.1	-112.9	C(30) - C(25) - C(24) - C(23)	73.0	-112.9
C(12) - C(15) - C(16) - C(17)	-75.3	63.1	C(28) - C(31) - C(32) - C(1)	-75.1	63.2
C(13) - C(12) - C(15) - C(16)	-96.3	-110.4	C(27) - C(28) - C(31) - C(32)	84.3	-110.6
C(11) - C(12) - C(15) - C(16)	84.2	68.9	C(29) - C(28) - C(31) - C(32)	-96.3	68.7
C(18) - C(17) - C(16) - C(15)	107.5	-81.3	C(2) - C(1) - C(32) - C(31)	107.4	-81.2
C(22) - C(17) - C(16) - C(15)	-72.8	99.0	C(6) - C(1) - C(32) - C(31)	-73.0	99.0

Both conformers have average D₂ symmetry. The conformer **1** is similar to the D_{2d} form and the conformer **2** is similar to the D₂ form in Wennerström et al. work [51] that has been denoted as (G⁺G⁻G⁺G⁻) and (G⁺G⁺G⁺G⁺), respectively. These conformations are shown in Figure 1b and the dihedral an-

gles are given in Table 1. The difference between the steric energy of **1** and **2** is 0.2 kcal·mol⁻¹, with **2** being higher in steric energy.

The guest molecules examined were CH₃X (X = H, F, Cl, Br, I) and CH_nCl_{4-n} (n = 0, 1, 2). The starting geometries for searching the potential energy surface (PES) of the interaction between each stable conformation of 4^o-PCP and the guest molecules were obtained by placing the guest at 10 Å apart from the host centre and then letting the guest come close to the host centre along the z-axis in 0.2 Å steps. The gravity centre of the guest was kept always on the z-axis, which is defined as the reaction coordinate. Once the guest molecule was approaching the host cavity, the guest was allowed to rotate in different directions to find out the best geometry for interaction with the host cavity. In this way the optimum geometry for each complex was found. Then the guest was taken away from the host cavity in the opposite direction of entrance to find out if this process could interconvert different conformations of 4^o-PCP.

Two types of complexes were found on the PES, one nesting [52], in which there is interaction between 4^o-PCP and guest, but the guest has not been introduced in the host cavity. In this case no important changes in 4^o-PCP geometry are seen. The other minimum energy on the PES is taken as inclusion complex as the guest is introduced to the host cavity. To simplify the analysis, the effect of entropy on the complex formation of the **1** and **2** conformations was considered similar; therefore the present analysis is based on the differ-

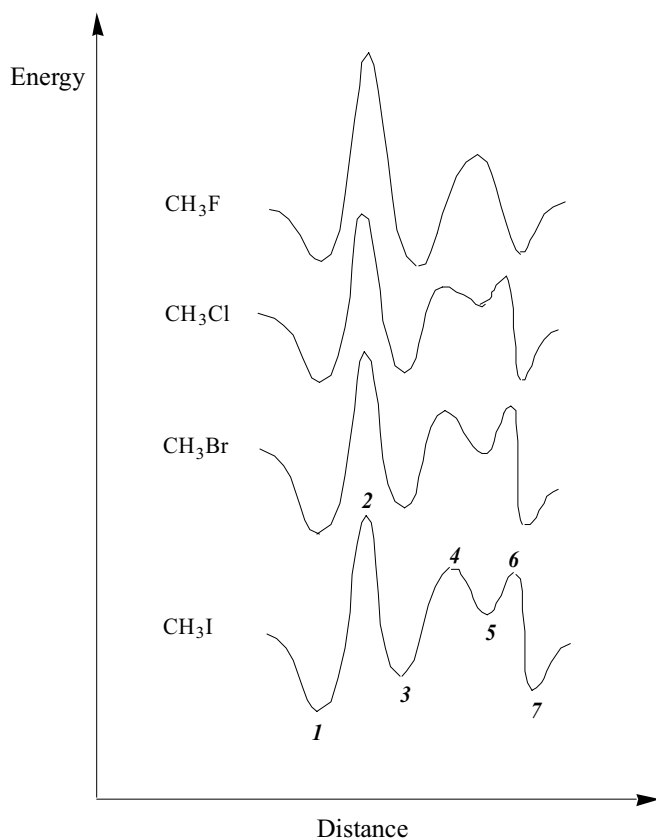


Figure 4 The PES of interaction of CH₃X as guest with the **1** cavity. The x-axis refers to the distance between the gravity centre of the guest molecules and the host centre. The y-axis shows an over view of the relative energies translated along the y-axis

Table 2 The E_p (kcal·mol⁻¹) for the energy minima and maxima of interaction of CH₃X with **1**. *Italic numbers refer to the energy minima and maxima given in Figure 4*

Guest	1	2	3	4	5	6	7
CH ₃ F	-2.3	4.6	-2.5	-	-	1.3	-2.0
CH ₃ Cl	-2.8	2.8	-2.5	0.3	-0.4	0.6	-2.7
CH ₃ Br	-3.5	2.6	-2.6	0.6	-0.8	0.7	-3.1
CH ₃ I	-3.9	2.7	-2.8	0.9	-0.7	0.7	-3.1

Table 3 Positional parameters (distances in Å and angles in degree) of CH_3X in its inclusion complex with **1**; for the numbering see Figure 7.

Guest		H_1	H_2	H_3	X
CH_3F	$\text{H}\cdots\pi$	2.81	2.89	2.82	3.03
	$\angle \text{C-H}\cdots\pi$	126.7	119.8	125.7	104.1
CH_3Cl	$\text{H}\cdots\pi$	2.74	2.94	2.76	3.49
	$\angle \text{C-H}\cdots\pi$	137.8	118.7	135.6	85.6
CH_3Br	$\text{H}\cdots\pi$	2.75	2.94	2.75	3.69
	$\angle \text{C-H}\cdots\pi$	138.4	120.0	140.7	79.67
CH_3I	$\text{H}\cdots\pi$	2.74	2.93	2.74	3.89
	$\angle \text{C-H}\cdots\pi$	142.6	122.0	139.9	74.1

ence in complexation energy (E_p). E_p is the difference in potential energies at infinite separation (zero energy) compared to that of a bound complex [53]. The use of molecular mechanics to estimate the complexation energies is assumed justified as the interaction of the guests with different conformations of the same host are investigated.

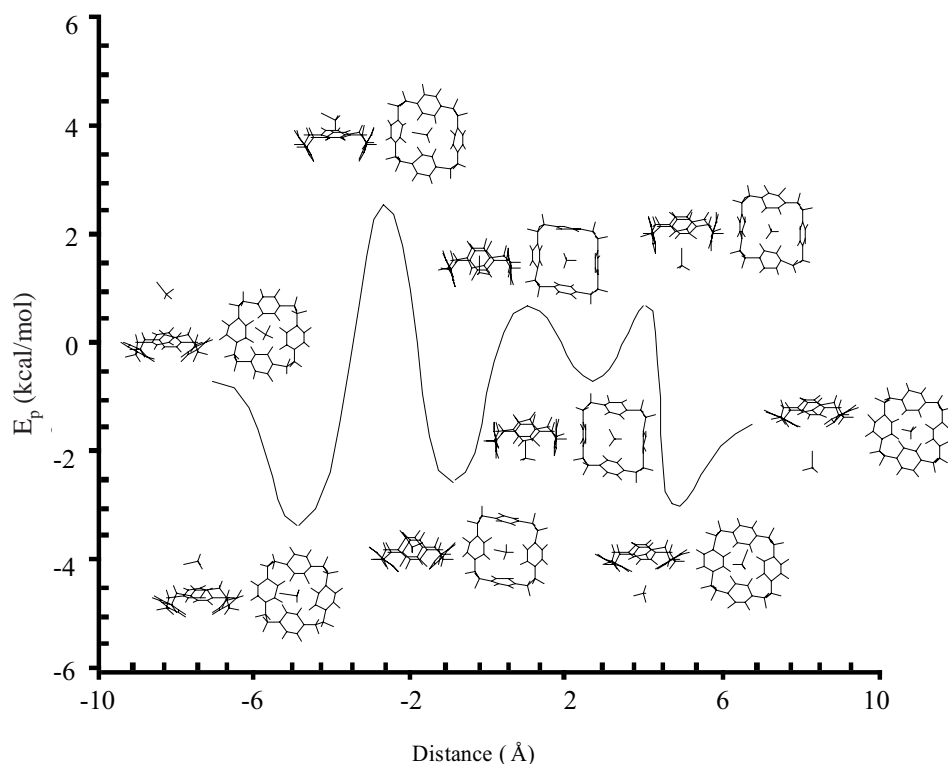
Results and discussion

The formation of nesting and inclusion complexes of several small organic molecules with the two lowest energy minimum conformations of 4°-PCP (**1** and **2**) is studied. The interaction between the two conformations of 4°-PCP with methane will be discussed in detail and for other guests the difference in behaviour compared to methane will be pre-

sented. The PESs for the complexation of methane in two conformations of 4°-PCP are shown in Figures 2 and 3.

Inclusion in **1** takes place in two distinct steps. The first one is the formation of a nesting complex in which the stabilising energy is attractive van der Waals with $E_p = -1.9$ kcal·mol⁻¹. The conformation of **1** does not change at this step, nor is there a barrier for the formation of the nesting complex. To get an inclusion complex, the guest is forced to enter the host cavity. This process needs reorganisation of the host to open up its cavity, so all benzene rings rotate when the guest enters in the cavity. This process causes a barrier of 8.2 kcal·mol⁻¹. Inclusion complex of **1** and methane is 0.4 kcal·mol⁻¹ more stable than the nesting complex. Here the change in E_p of inclusion compared to the nesting is mostly due to van der Waals interactions. Although the host conformation **1** in the inclusion complex has remained similar to its initial optimised geometry, changes in dihedral angles have

Figure 5 The potential energy surface of interaction of CH_3Br as guest with **1**. Two different views are given for each minimum and maximum energy structure.



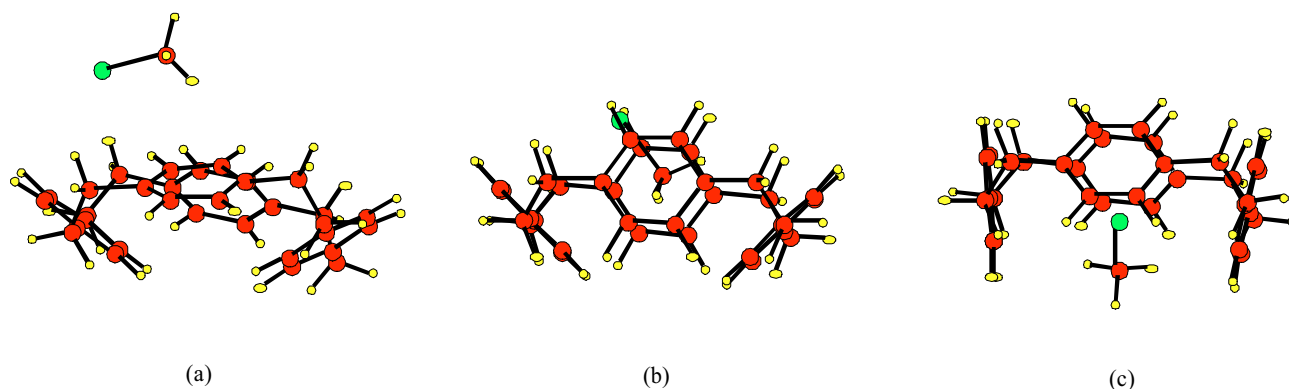


Figure 6 The calculated structures of (a) the nesting complex, (b) the first inclusion complex and (c) the second inclusion complex of CH_3Br with the cavity of **1**

occurred without any important changes in the other structural parameters.

Decomplexation of the inclusion complex of **1** and methane could occur either by a reverse process or by forcing the guest to come out from the other side of the host cavity. The barrier for the second process is less than the first one ($4.1 \text{ kcal}\cdot\text{mol}^{-1}$ compared to the inclusion complex), so two lateral benzene rings will rotate to let the guest exit from the cavity.

Another nesting complex will form when guest exits the host cavity from the other side. This nesting complex is located $0.2 \text{ kcal}\cdot\text{mol}^{-1}$ higher than the first nesting complex,

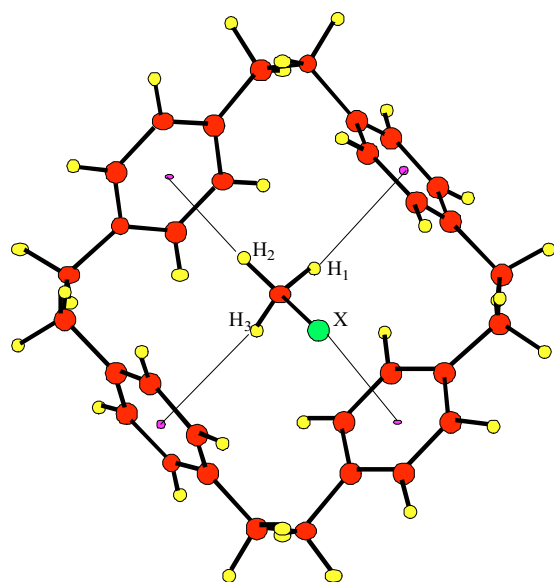


Figure 7 The optimum structure of inclusion complex of CH_3X with **1** as calculated by MMP2(87). H_1 and H_3 are closer to the π -face of the aromatic rings, while H_2 is on a longer distance.

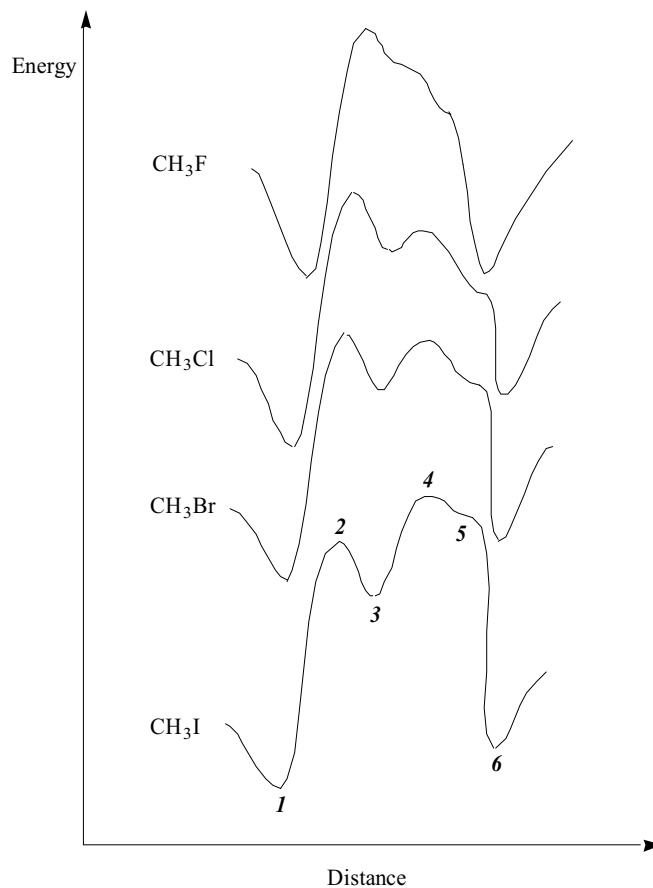


Figure 8 The potential energy surfaces of interaction of CH_3X as guest with the cavity of **2**. The x-axis refers to the distance between the gravity centre of the guest molecules and the host centre. The y-axis shows an over view of the relative energies translated along the y-axis

Table 4 The E_p (kcal·mol⁻¹) of the energy minima and maxima of interaction of CH₃X with **2**. *Italic numbers refer to the energy minima and maxima given in Figure 8.*

Guest	<i>1</i>	<i>2</i>	<i>3</i>	<i>4</i>	<i>5</i>	<i>6</i>
CH ₃ F	-4.9	1.2	0.2	0.6	-0.9	-3.6
CH ₃ Cl	-5.1	1.6	0.1	0.6	-0.9	-3.8
CH ₃ Br	-5.6	1.0	-0.5	0.8	-0.1	-4.4
CH ₃ I	-6.0	0.5	-0.9	1.3	1.4	-4.9

Table 5 Positional parameters (distances in Å and angles in degree) of CH₃X in its inclusion complex with **2**; for the numbering see Figure 11.

Guest		H ₁	H ₂	H ₃	X
CH ₃ F	H···π	2.85	2.69	2.56	4.08
	∠C-H···π	139.6	112.2	151.0	60.9
CH ₃ Cl	H···π	2.86	2.75	2.63	3.86
	∠C-H···π	138.9	113.6	142.0	67.1
CH ₃ Br	H···π	2.97	2.76	2.73	3.47
	∠C-H···π	128.5	112.5	129.5	81.1
CH ₃ I	H···π	2.85	2.81	2.54	4.28
	∠C-H···π	142.5	111.5	154.7	56.3

see Figure 2. The E_p is higher because of the difference in orientation of the guest to the host cavity and a small difference between 4°-PCP conformations in these two nesting complexes. However, full optimisation will result in the same nesting complex.

Complex formation between conformation **2** and CH₄ as a guest is interesting as the nesting complex is lower in energy than the inclusion one by 6.0 kcal·mol⁻¹, see Figure 3. Formation of the inclusion complex needs the reorganisation of the host molecule. This will happen by a barrier of 7.2 kcal·mol⁻¹ relative to the nesting complex. In this case forcing the guest to exit from the other side of host does not need much energy (less than 0.1 kcal·mol⁻¹ relative to the inclusion complex, see Figure 3). It seems that with **2** the nesting complex is the preferred one.

The difference between the E_p of inclusion complex of **1** and the nesting complex of **2** with methane is 1.2 kcal·mol⁻¹. Therefore, the nesting one with **2** is more stable. Hence, the preference of 4°-PCP for the **2** conformation in solution might be explained on this basis.

Figure 9 The potential energy surface of interaction of CH₃Cl as guest with **2**. The top and side views of the minimum and maximum energy structures are given.

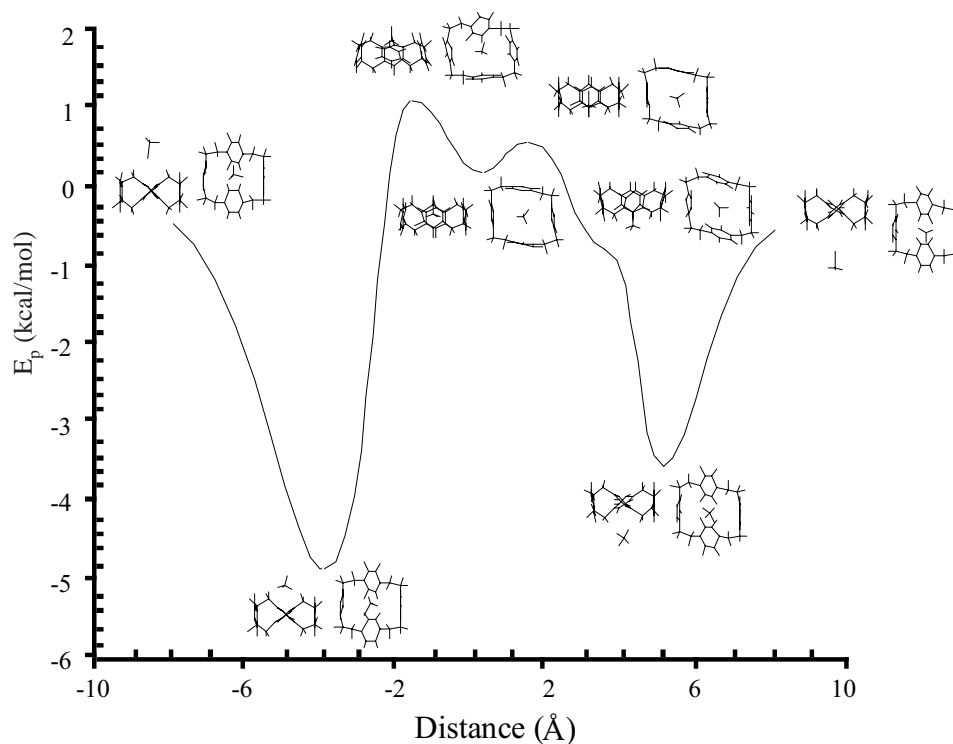


Table 6 The E_p ($\text{kcal}\cdot\text{mol}^{-1}$) of the energy minima and maxima of interaction of $\text{CH}_n\text{X}_{4-n}$ with **1**. *Italic numbers refer to the energy minima and maxima given in Figure 12.*

Guest	<i>1</i>	<i>2</i>	<i>3</i>	<i>4</i>	<i>5</i>	<i>6</i>	<i>7</i>
CH_3Cl	-2.8	2.8	-2.5	0.3	-0.4	0.6	-2.7
CH_2Cl_2	-3.3	2.0	-3.4	11.3	-1.4	0.7	-2.5
CHCl_3	-4.1	3.4	1.0	12.8	-2.5	-1.3	-2.8
CCl_4	-3.5	1.5	-0.5	21.5	-1.6	-0.9	-3.5

Complex formation of several mono-substituted methanes was examined with **1** and **2**. CH_3F behaves like CH_4 but other mono-substituted methanes show additional local minima on the PES for the conformation **1**, see Figure 4 and Table 2. It is noteworthy that at the beginning, the guest (CH_3X) sits in the host cavity of **1** from the three hydrogen umbrella side, see Figure 5. This will result in the first nesting complex. Also, the first inclusion complex forms with the same orientation of CH_3X with the host cavity, see Figure 6a and 6b. When the guest is forced to go through the host cavity, a change in the guest orientation relative to the host cavity happens and the second inclusion complex forms, this time with the X-substituent located in the centre of the host cavity, see Figures 5 and 6c. Forcing the guest further to exit from the cavity will result in obtaining a nesting complex quite similar to the first nesting one, with a bit higher E_p as found with **1** and methane, see Figure 5.

It is interesting to mention that in the inclusion complexes of mono-substituted methanes with **1**, all three hydrogen atoms were found pointing on the face of the benzene rings. Two hydrogen atoms are closer to the face of the aromatic rings and the third one with a longer distance, see Figure 7 and Table 3. By changing X from F to I in CH_3X , the hydrogen atom distances from the π -face of benzene rings decrease. This is probably due to an increase in the halogen size, which force the hydrogen atoms to go further down in the host cavity until the whole molecule fits properly in the host cavity. Another point noteworthy on the PES of the interaction of mono-substituted methanes with **1** is the fact that the nesting complex is lower in energy than the inclusion one except in CH_3F , see Figure 4 and Table 2.

For **2**, the nesting complexes with CH_3X are always lower in energy than the inclusion ones as found in methane, see Figure 8 and Table 4. Two kinds of nesting complexes form by interaction of **2** with CH_3X . The first nesting complex with **2** forms by interaction of the X- substituent as well as two hydrogen atoms with the host cavity. The second one forms by a change in the orientation of CH_3X relative to the cavity so that the three hydrogen atoms come to contact with the host cavity. The reason for this behaviour might be explained as follows. The host cavity in **2** is more available than in **1**. When CH_3X approaches the host surface in **2**, the negative end of the C-X bond dipole interacts with the positive end of the bond dipoles located on the aromatic C-H's to form the first nesting complex. Once the CH_3X comes closer to the

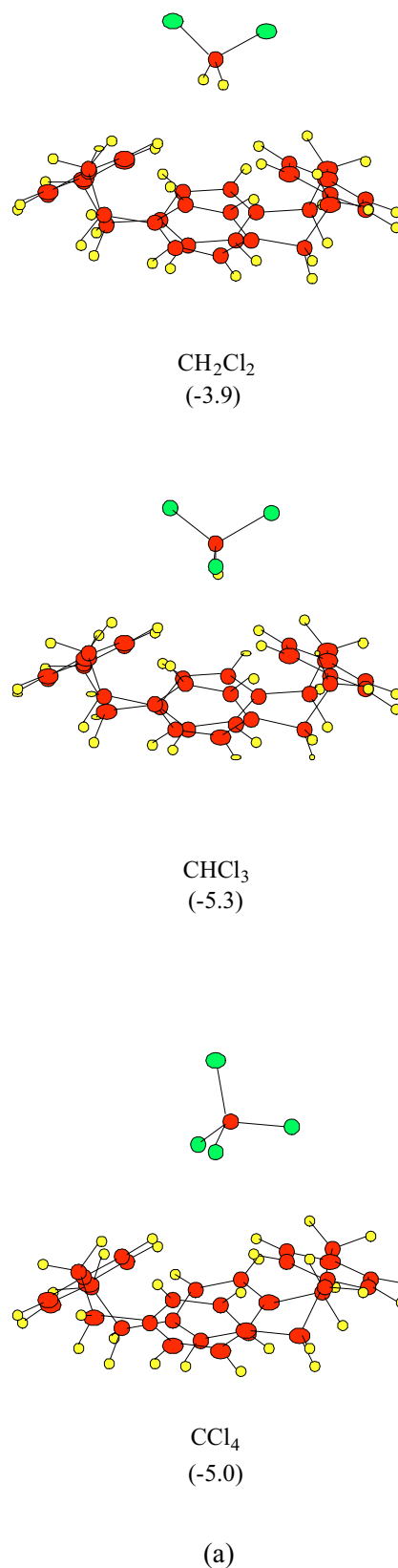
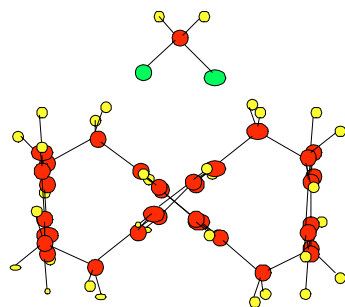
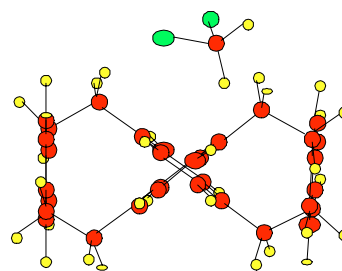


Figure 10a The optimised structure of the nesting complexes of CH_2Cl_2 , CHCl_3 , CCl_4 with the cavity of **1**. The E_p in $\text{kcal}\cdot\text{mol}^{-1}$ for each is given in parentheses.

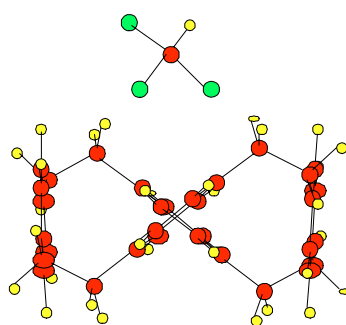
Figure 10b The calculated structures of the nesting complexes of CH_2Cl_2 , CHCl_3 and CCl_4 with the cavity of **2**. The E_p in kcal mol^{-1} for each is given in parentheses.



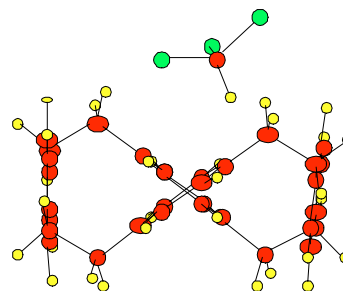
CH_2Cl_2
(-6.0)
C-Cl nesting



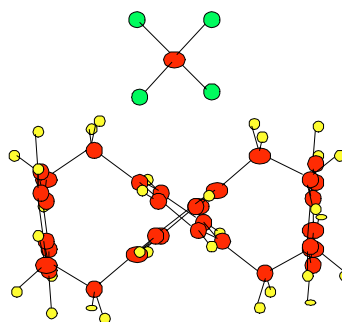
CH_2Cl_2
(-6.8)
C-H nesting



CHCl_3
(-7.0)
C-Cl nesting



CHCl_3
(-7.5)
C-H nesting



CCl_4
(-7.7)

(b)

cavity of **2**, the repulsive interactions of the C-X bond dipole and the aromatic π system leads to the reorientation of the guest. Now the positive ends of the C-H bond dipoles of CH_3X interact with the aromatic π system to form the second nesting complex, see Figure 9.

This is much pronounced when the formation of the nesting complexes of **2** with CH_2Cl_2 and CHCl_3 are studied, where in both chlorine atoms come to contact with the host cavity at first. CH_2Cl_2 comes in contact with the cavity of **2** by its Cl atoms to form the first nesting complex. Then at a closer distance, the guest reorientation toward the host cavity happens and one of the hydrogen atoms sits in the cavity of **2** to form the second nesting complex; with CHCl_3 as a guest, similar behaviour is seen, see Figure 10b.

The first inclusion complex of CH_3X with **2** forms by large changes in dihedral angles of **2**. This causes the inclusion complex to be higher in energy than the nesting one. In the first inclusion complex of CH_3X with **2**, the hydrogen atoms were found close to the π -face of aromatic rings, although they were in a bent direction, see Figure 11 and Table 5.

The barrier against exiting from the other side of host in **2** is quite low. During the exit, another inclusion complex seems to form on the PES, see Figure 9. For CH_3Cl , this complex is not deep in energy compared to the transition state connecting this to the last nesting complex formed on the PES. The difference between the inclusion complexes with **2** is due to the difference in orientation of the guest toward the host cavity. The last energy minimum on the PES that is related to

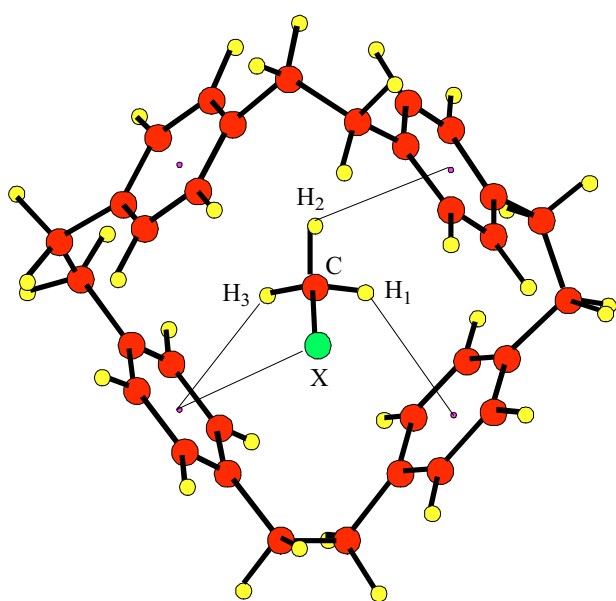


Figure 11 The optimized structure of the first inclusion complex of CH_3X with **2** as calculated by MMP2(87). H_3 is closer to the π -face of the aromatic ring, while H_1 and H_2 are on the longer distances.

the formation of a nesting complex is similar to the first nesting complex, but with higher E_p . This is because of the difference in the geometry of **2** compared with the starting geometry, see Figure 9.

Deuterated chloroform and deuterated dichloromethane are used as solvent for dynamic NMR measurements from the ambient temperature down to -50°C and -80°C , respectively [54]. Interaction of these solvents as guests with the host molecules like 4°-PCP may affect the conformational preferences in 4°-PCP . Therefore interactions of these molecules and CCl_4 with **1** and **2** were examined.

It was found that the nesting and inclusion complexes of CH_2Cl_2 with **1** have the same energy, but for CHCl_3 and CCl_4 the nesting complexes are more stable by $3 \text{ kcal}\cdot\text{mol}^{-1}$ than the inclusion ones, see Figure 12 and Table 6. Forcing CH_2Cl_2 , CHCl_3 and CCl_4 to pass through the cavity of **1** is a very high-energy process.

The less stable conformation of 4°-PCP , **2**, will form only nesting complexes with CH_2Cl_2 , CHCl_3 and CCl_4 . The dif-

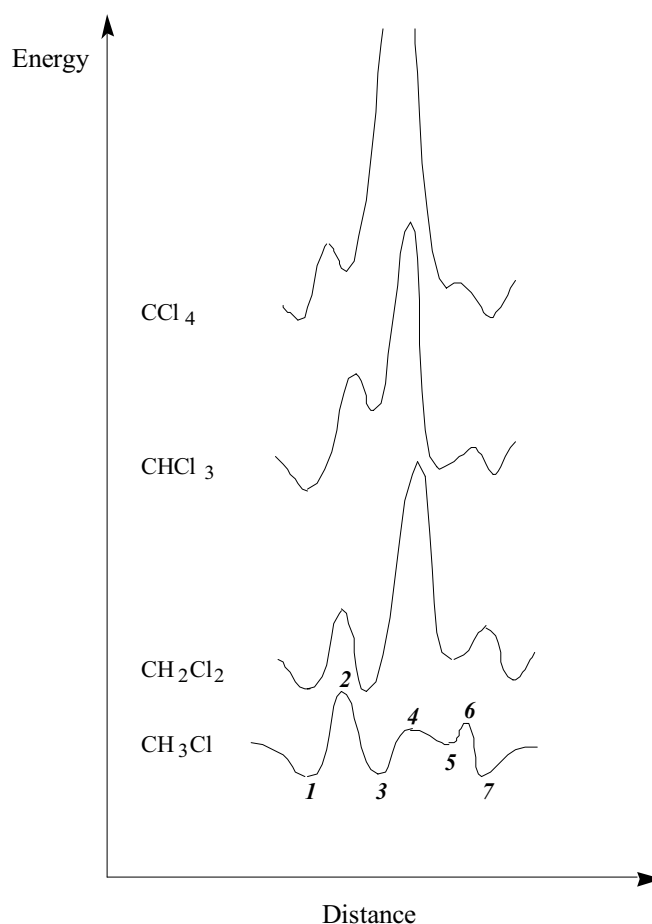


Figure 12 The potential energy surfaces of interaction of $\text{CH}_n\text{X}_{4-n}$ as guest with the cavity of **1**. The x-axis refers to the distance between the gravity centre of the guest molecules and the host centre. The y-axis shows an over view of the relative energies translated along the y-axis.

ferences between the nesting and inclusion complexes were found to be more than $16 \text{ kcal}\cdot\text{mol}^{-1}$. With CH_2Cl_2 and CHCl_3 , two types of nesting complexes form on the PES, the C-Cl nesting in which C-Cl ends of the solvent molecule are located toward the aromatic C-H's and the C-H nesting in which the C-H is located toward the π -faces of the aromatic rings. With the CH_2Cl_2 and CHCl_3 as guests, the C-H nesting complexes were found to be 0.8 and $0.5 \text{ kcal}\cdot\text{mol}^{-1}$ more stable than the C-Cl nesting complexes, respectively. Since, the barrier against the conversion of C-Cl to C-H nesting were found $2.1 \text{ kcal}\cdot\text{mol}^{-1}$ for CH_2Cl_2 and $4.6 \text{ kcal}\cdot\text{mol}^{-1}$ for CHCl_3 , we have chosen the energies of the first nesting complexes in **1** and **2** and have compared them, as there is no barrier against their formations.

The C-Cl nesting complexes of CH_2Cl_2 , CHCl_3 and CCl_4 with **2** were found 2.1 , 1.7 and $2.8 \text{ kcal}\cdot\text{mol}^{-1}$ lower in energy than the nesting complexes with **1**, respectively, see Figures 10a and 10b. It seems that with such solvents a nesting complex should be formed with **2**. This affects the population equilibrium of $\mathbf{1} \leftrightarrow \mathbf{2}$ quite dramatically. The difference in steric energies of **1** and **2** is only $0.2 \text{ kcal}\cdot\text{mol}^{-1}$. Therefore, it is expected that both should be populated in similar ratio at the gas phase, but due to the nesting interactions with solvents, **2** should be more populated than **1** in solution. At lower temperatures, where the difference between the energy of the nesting complexes of **1** and **2** is more important, this phenomenon is especially favoured.

One possibility is that two solvent molecules interact at the same time with the host cavity, in this case a double nesting complex with both molecules sat on the opposite sides of the host could be formed. Therefore the formation of double nesting complexes of CH_2Cl_2 , CHCl_3 and CCl_4 with **1** and **2** were studied. The double nesting of **1** with CH_2Cl_2 , i.e. $\mathbf{1}:2 \text{ CH}_2\text{Cl}_2$, is less stable than the double nesting complex of **2** with CH_2Cl_2 , i.e. $\mathbf{2}:2 \text{ CH}_2\text{Cl}_2$, by $3.8 \text{ kcal}\cdot\text{mol}^{-1}$. The difference between $\mathbf{1}:2 \text{ CHCl}_3$ and $\mathbf{2}:2 \text{ CHCl}_3$ is $3.4 \text{ kcal}\cdot\text{mol}^{-1}$ and the difference between $\mathbf{1}:2 \text{ CCl}_4$ and $\mathbf{2}:2 \text{ CCl}_4$ is estimated to be $3.7 \text{ kcal}\cdot\text{mol}^{-1}$, so in all cases the double nesting with **2** is predicted to be more stable, see Figure 13a and 13b. In both cases (nesting and double nesting) it seems that interaction of solvent molecules with 4° -PCP cavity will result in the dominant population of the **2** conformer in solution, although **2** is less stable than **1** by $0.2 \text{ kcal}\cdot\text{mol}^{-1}$ in the gas phase. Wennerström et al. [52] based on the analysis of ^1H NMR spectrum of 4° -PCP at low temperatures and taking into account the result of Tabushi et al. [55,56] dynamic NMR measurements on the substituted 4° -PCP concluded that **2** is the preferred conformation in solution.

Conclusion

Force field calculations are used to calculate the interaction energies of different guest molecules with the two lowest energy minima conformations of 4° -PCP, **1** and **2**. It is found that the formation of a nesting and a double nesting type of complexes between **1** and **2** and the solvent molecules could be taken into account to explain the preference of the **2** over **1**

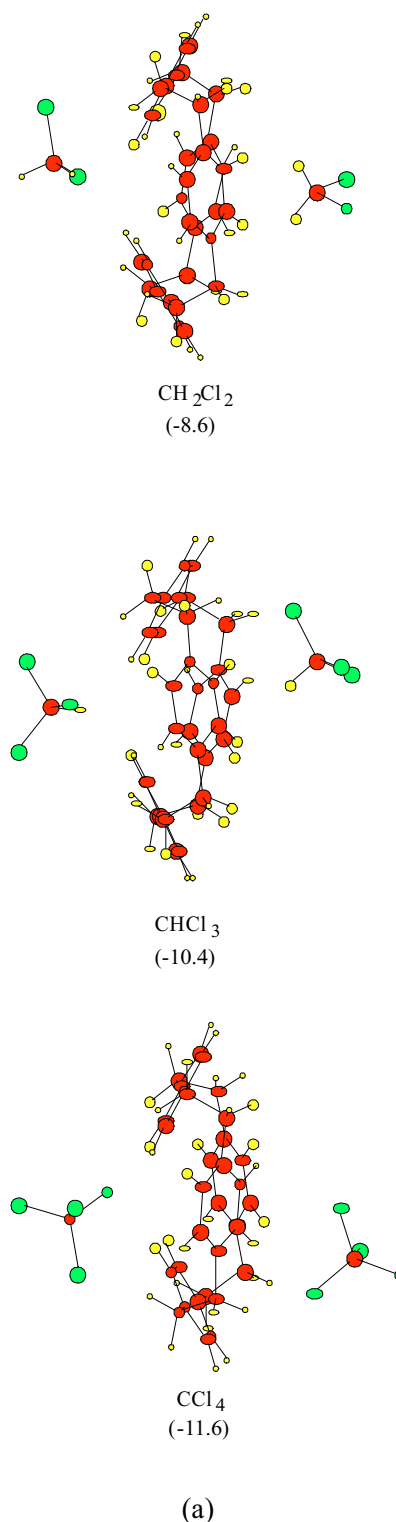
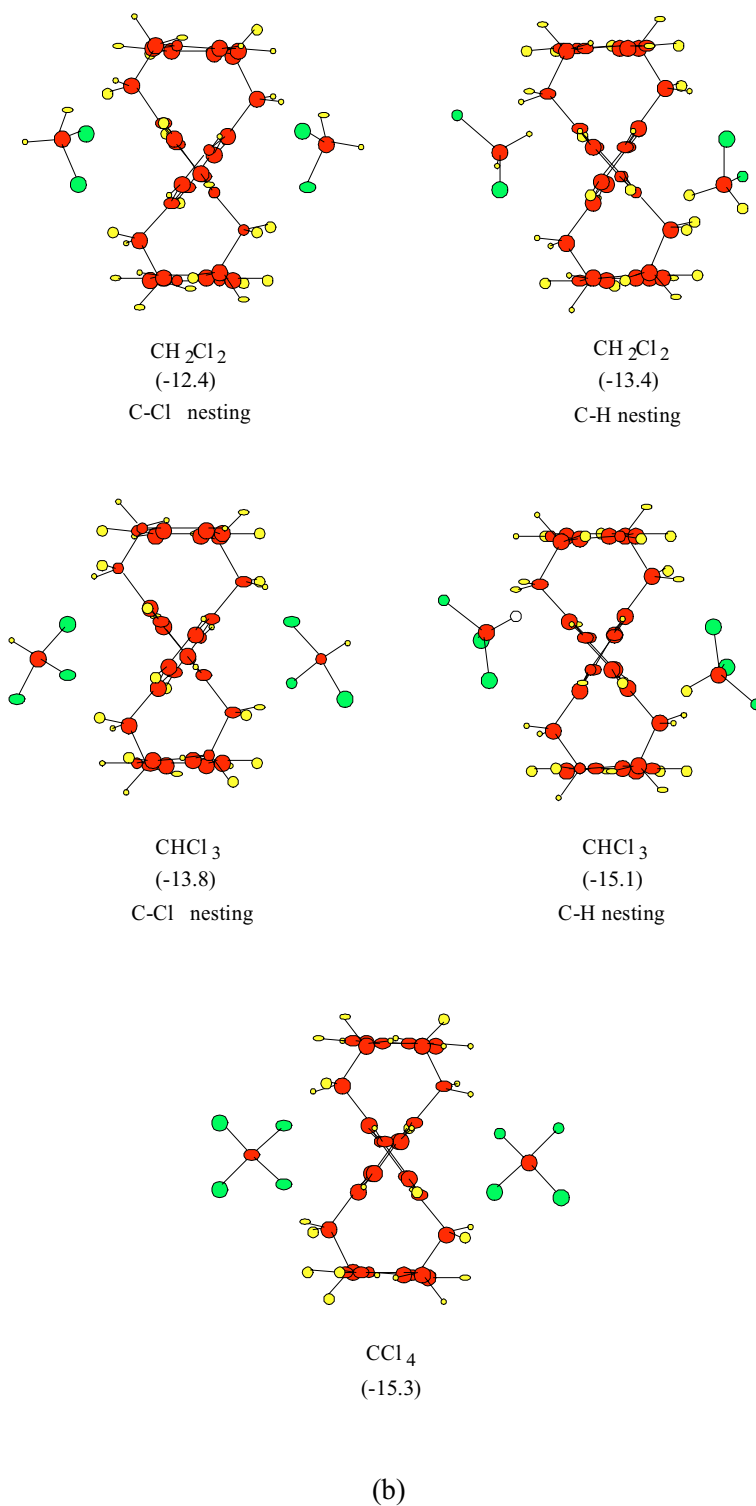


Figure 13a The optimised structure of the double nesting complexes of two $\text{CH}_n\text{Cl}_{4-n}$ molecules with the cavity of **1**. E_p 's in $\text{kcal}\cdot\text{mol}^{-1}$ are given in parentheses.

Figure 13b The optimised structure of the double nesting complexes of two $\text{CH}_n\text{Cl}_{4-n}$ molecules with the cavity of **2**. E_p 's in $\text{kcal}\cdot\text{mol}^{-1}$ are given in parentheses.



in solution; although in the gas phase the steric energy of **1** is estimated to be $0.2 \text{ kcal}\cdot\text{mol}^{-1}$ lower than **2**. Wennerström et al. [52] have suggested the **2** form as the dominant one in solution.

Acknowledgement We are grateful to the Research Council of Tehran University for financial support.

Supplementary Material Available Cartesian coordinates for all stationary points as calculated by MM2(87) programme are available in PDB format.

References

1. Cram, D. J. *Acc. Chem. Res.* **1978**, *11*, 8.
2. Cram, D. J.; Cram, J. M. *Container Molecules and Their Guests*, Royal Society of Chemistry; Cambridge, England, 1994.
3. Cram, D. J. *Nature* **1992**, *356*, 29.
4. Lehn, J. M. *Comprehensive Supramolecular Chemistry*, 1st ed., Elsevier Science Inc., New York, 1996, **2**, pp.69-101 and **4**, pp.2, 4-8.
5. Lehn, J. M. *Angew. Chem., Int. Ed. Engl.* **1989**, *27*, 89.
6. Lehn, J. M. *Angew. Chem., Int. Ed. Engl.* **1990**, *29*, 1304.
7. Cram, D. J. *Angew. Chem., Int. Ed. Engl.* **1988**, *27*, 1009.
8. Tabushi, I.; Yamamura, K.; Nonoguchi, H.; Hirotsu, K.; Higuchi, T. *J. Am. Chem. Soc.* **1984**, *106*, 2621.
9. Tabushi, I.; Yamamura, K.; Nonoguchi, H.; Hirotsu, K.; Higuchi, T.; Kamitori, S. *J. Incl. Phenom.* **1984**, *2*, 215.
10. Böhmer, V.; Ferguson, G.; Gallagher, J. F.; Lough, A. J.; McKervey, M. A.; Madigan, E.; Moran, M. B.; Phillips, J.; Williams, G. J. *J. Chem. Soc., Perkin Trans. 1* **1993**, 1521.
11. Ferguson, G.; Gallagher, J. F.; Li, Y.; McKervey, M. A.; Madigan, E.; Moran, M. B.; Malone, J. F.; Walker, A. *Supramol. Chem.* **1996**, *7*, 223.
12. Atwood, J. L.; Bott, S. G.; Jones, C.; Raston, C. L. *J. Chem. Soc., Chem. Commun.* **1992**, 1349.
13. Diederich, F. *Angew. Chem., Int. Ed. Engl.* **1988**, *27*, 362.
14. Houk, K. N.; Diederich, F.; Ferguson, S. B.; Carcanague, D. R.; Evanseck, J. D.; Smithrud, D. B.; Sanford, E. M.; Chao, I. *Pure Appl. Chem.* **1990**, *62*, 2227.
15. Adams, S. P.; Whitlock, H. W. *J. Am. Chem. Soc.* **1982**, *104*, 1602.
16. Jarvi, E. T.; Whitlock, H. W. *J. Am. Chem. Soc.* **1982**, *104*, 7196.
17. Inazu, T.; Nishikido, J.; Yoshino, T. *Bull. Chem. Soc. Jpn.* **1973**, *46*, 263.
18. Inazu, T.; Nishikido, J.; Yoshino, T. *Bull. Chem. Soc. Jpn.* **1973**, *46*, 653.
19. Inazu, T.; Yoshino, T. *Bull. Chem. Soc. Jpn.* **1968**, *41*, 652.
20. Koga, K.; Itai, A.; Iitaka, Y.; Odashima, K. *J. Am. Chem. Soc.* **1980**, *102*, 2504.
21. Diederich, F.; Griebel, D. *J. Am. Chem. Soc.* **1984**, *106*, 8037.
22. Vögtle, F.; Wallon, A.; Werner, U.; Müller, M. W.; Nieger, M. *Chem. Ber.* **1990**, *123*, 859.
23. Whitlock, H. W.; Whitlock, B. J. *J. Am. Chem. Soc.* **1994**, *116*, 2301.
24. Janzen, E. G.; Diederich, F. N.; Sanford, E. M.; Kotake, Y. *J. Org. Chem.* **1989**, *54*, 5421.
25. Jorgensen, W. L. *Acc. Chem. Res.* **1989**, *22*, 184.
26. Houk, K. N.; Diederich, F.; Ferguson, S. B.; Seward, E.; Brown, F. K.; Loncharich, R. J. *J. Org. Chem.* **1988**, *53*, 3479.
27. Houk, K. N.; Sheu, C. *J. Am. Chem. Soc.* **1996**, *118*, 8056.
28. Jaime, C.; Pérez, F.; Ruiz, S. *J. Org. Chem.* **1995**, *60*, 3840.
29. Dong, S.-J.; Zhang, D.-B.; Lü, T.-X. *J. Chem. Soc., Faraday Trans. 2*, **1989**, *85*, 1439.
30. Jaime, C.; Ivanov, P. M. *An. Quim. Int. Ed.* **1996**, *92*, 13.
31. Cogorden, J. A.; Lara - Ochoa, F.; Silaghi - Dumitrescu, I. *Fullerene Sci. Technol.* **1996**, *4*, 887.
32. Chin, D. H.; Gordon, D. M.; Whitesides, G. M. *J. Am. Chem. Soc.* **1994**, *116*, 12033.
33. Jorgensen, W. L.; Nguyen, T. B.; Sanford, E. M.; Chao, I.; Houk, K. N.; Diederich, F. *J. Am. Chem. Soc.* **1992**, *114*, 4003.
34. Pranata, J.; Jorgensen, W. L. *J. Am. Chem. Soc.* **1991**, *113*, 9483.
35. Pranata, J.; Jorgensen, W. L. *J. Am. Chem. Soc.* **1990**, *112*, 2008.
36. Pranata, J.; Jorgensen, W. L. Wierschke, S. G. *J. Am. Chem. Soc.* **1991**, *113*, 2810.
37. Guilbaud, P.; Varnek, A.; Wipff, G. *J. Am. Chem. Soc.* **1993**, *115*, 8298.
38. Lipkowitz, K. B. *Chem. Rev.* **1998**, *95*, 1829.
39. Iwamoto, K.; Ikeda, A.; Araki, K.; Harada, T.; Shinkai, S. *Tetrahedron* **1993**, *49*, 9937.
40. Rashidi-Ranjbar, P.; Taqvaie, S. *manuscript in preparation*.
41. Reinhoudt, D. N.; van Hoorn, W. P.; Briels, W. J.; van Duynhoven, J. P. M.; van Veggel, F. C. J. M. *J. Org. Chem.* **1998**, *63*, 1299.
42. Reinhoudt, D. N.; Groenen, L. C.; Steinwender, E.; Lutz, B. T. G.; van der Maas, J. *J. Chem. Soc., Perkin Trans 2* **1992**, 1893.
43. Chapman, K. T.; Still, W. C. *J. Am. Chem. Soc.* **1989**, *111*, 3075.
44. Sheridan, R. E.; Whitlock, H. W. *J. Am. Chem. Soc.* **1986**, *108*, 7120.
45. Diederich, F.; Dick, K.; Griebel, D. J. *J. Am. Chem. Soc.* **1986**, *108*, 2273.
46. Liljefors, T.; Tai, J.; Li, S.; Allinger, N. L. *J. Comput. Chem.* **1987**, *8*, 1051.
47. Allinger, N. L.; Burkert, U. *Molecular Mechanics*, American Chemical Society, Washington, DC 1982.
48. Liljefors, T.; Norrby, P.-O.; Pettersson, I.; Gundertofte, K. *J. Comput. Chem.* **1996**, *17*, 429.
49. Rashidi-Ranjbar, P.; Arshadi, N. *manuscript in preparation*.
50. Cristol, S. J.; Lewis, D. C. *J. Am. Chem. Soc.* **1967**, *89*, 1476.
51. Wennerström, O.; Tanner, D.; Thulin, B.; and Olsson, T. *Tetrahedron* **1981**, *37*, 3473.
52. Tabushi, I.; Kimura, Y.; Yammamura, K. *J. Am. Chem. Soc.* **1981**, *103*, 6486.
53. Pang, L.; Whitehead, M. A. *Supramol. Chem.* **1992**, *1*, 81.
54. Sandstrom, J. *Dynamic NMR Spectroscopy*, Academic Press, London, 1982.
55. Tabushi, I.; Yamada, H.; and Kuroda, Y. *J. Org. Chem.* **1975**, *40*, 1946.
56. Tabushi, I.; Yamada, H. *Tetrahedron* **1977**, *33*, 1101.